

Lab Report

**S261: Optical Astronomy and Gravitational
Lensing**

Chenhuan Wang and Harilal Bhattacharai

September 18, 2020

1. Lensing

1.1. Background*

1.1.1. Cosmic Expansion

A spatially homogeneous and isotropic Universe can be described as FLRW metric. Solving Einstein's field equations with FLRW metric gives expansion of the Universe [2]. Hubble parameter $H(t) = \dot{a}(t)/a(t)$ evolves according to

$$H^2(t) = H_0^2 [\Omega_{\text{rad}} a^{-4}(t) + \Omega_{\text{mat}} a^{-3}(t) + \Omega_{\text{curv}} a^{-2}(t) + \Omega_\Lambda] \quad (1.1)$$

Because of expansion of the Universe, light emitted in the past gets redshifted over time. The redshift of a source is given by,

$$z = \frac{\lambda_{\text{obj}} - \lambda_{\text{em}}}{\lambda_{\text{em}}} \quad (1.2)$$

Where, λ_{obs} and λ_{em} are, respectively, the wavelengths at time of observation and emission. Redshift is directly related to the scale factor by,

$$1 + z = \frac{1}{a(t_{\text{em}})} \quad (1.3)$$

with scale factor at present time defined as $a(t_0) = 1$.

The local Hubble law are given by the following formula,

$$v_{\text{esc}} = H_0 D \quad (1.4)$$

where, $H_0 = H(t_0)$ is Hubble constant and D is the distance between object and observer.

1.1.2. Distances

Accordingly, one defines the angular diameter distance as exactly this ratio,

$$D_{\text{ang}}(z) = 2R/\delta = a(z)f_K(w) \quad (1.5)$$

Where, R is the radius of the distant object, δ is the angular diameter, and z is the cosmological redshift. If we consider an observer at redshift z_1 gives the angular diameter of another object at redshift z_2 , so equation 1.5 becomes

$$D_{\text{ang}}(z_1, z_2) = a(z_2)f_K[w(z_2) - w(z_1)] \quad (1.6)$$

Another distance measure relates the observed flux, S , of a source to its luminosity, L . For a known luminosity, the distance to the source can be determined as,

$$D_{\text{lum}}(z) = \sqrt{\frac{L}{4\pi S}} \quad (1.7)$$

*Content taken from [1], if not noted otherwise.

1.1.3. Quasars

1.1.4. Gravitational lensing

Figure 1.1.: Schematic diagram of the gravitational lensing system [wiki]. [picture and citation missing!](#)

Lens Equation

For simplicity, we assume that all angles considered are small so that $\tan x \approx \sin x \approx x$, source plane and lens plane are parallel, and light travels in straight line in between planes. For a given source, the lens equation is given by,

$$\boldsymbol{\beta} = \boldsymbol{\theta} - \boldsymbol{\alpha}(\boldsymbol{\theta}) \quad (1.8)$$

where, $\boldsymbol{\theta}$ is the apparent angular position of the source in the sky, $\boldsymbol{\beta}$ is its true position, and $\boldsymbol{\alpha}$ is the scaled deflection angle.

Now, we can define a dimensionless surface mass density with convergence as,

$$\kappa(\boldsymbol{\theta}) = \frac{\sum(D_d\boldsymbol{\theta})}{\sum_{\text{cr}}} \quad (1.9)$$

with the critical surface mass density,

$$\Sigma_{\text{cr}} = \frac{c^2}{4\pi G} \frac{D_s}{D_d D_{ds}} \quad (1.10)$$

The scaled deflection angle can be rewritten as,

$$\boldsymbol{\alpha}(\boldsymbol{\theta}) = \frac{1}{\pi} \int d^2\boldsymbol{\theta}' \kappa(\boldsymbol{\theta}') \frac{\boldsymbol{\theta} - \boldsymbol{\theta}'}{|\boldsymbol{\theta} - \boldsymbol{\theta}'|^2} \quad (1.11)$$

For further convenience, a deflection potential is introduced

$$\psi(\boldsymbol{\theta}) = \frac{1}{\pi} \int d^2\boldsymbol{\theta}' \kappa(\boldsymbol{\theta}') \ln |\boldsymbol{\theta} - \boldsymbol{\theta}'| \quad (1.12)$$

The use of this quantity is well-motivated because it encloses all information of the mass distribution of the lens [1]. In addition, relation of deflection potential and deflection angle can be found

$$\boldsymbol{\alpha}(\boldsymbol{\theta}) = \nabla \psi(\boldsymbol{\theta}) \quad (1.13)$$

From the deflection potential a further scalar function, the Fermat potential, can be defined

$$\tau(\boldsymbol{\theta}; \boldsymbol{\beta}) = \frac{1}{2} (\boldsymbol{\beta} - \boldsymbol{\theta})^2 - \psi(\boldsymbol{\theta}) \quad (1.14)$$

Finally to find the magnification of the images is given by

$$\mu = (\det A)^{-1} \quad (1.15)$$

where, A is the Jacobian matrix of lens mapping.

$$A_{ij} = \frac{\partial \beta_i}{\partial \theta_j} \quad (1.16)$$

The SIS (Singular Isothermal Sphere)

A simple model to describe the mass distribution of a galaxy acting as a lens is the singular isothermal sphere (SIS):

$$\rho(r) = \frac{\sigma_v^2}{2\pi Gr^2} \quad (1.17)$$

where σ_v is the velocity dispersion. Physically this means that the lens system consists of self-gravitating with Maxwellian velocity distribution [3].

Integration along the line of sight yields the surface mass density

$$\Sigma(\xi) = \frac{\sigma_v^2}{2G\xi} \quad (1.18)$$

A characteristic angular scale of an axisymmetric lens is given by the Einstein radius θ_E , defined as the angle inside which the mean of the convergence is unity. As a consequence, the projected mass inside θ_E can be written as,

$$M(\theta \leq \theta_E) = \pi \theta_E^2 D_d^2 \Sigma_{cr} \quad (1.19)$$

For an SIS the Einstein radius reads

$$\theta_E = 4\pi \left(\frac{\sigma_v}{c} \right)^2 \frac{D_{ds}}{D_s} \quad (1.20)$$

1.1.5. Calibration frames

1.1.6. Image reduction

1.2. Preparatory Tasks

P.3.1 Calculation of the deflection potential, $\psi(\theta)$ and the scaled deflection angle of an SIS lens.

From equation 1.12 the deflection potential, which gives the information about the mass distribution of the lens, is define as,

$$\psi(\theta) = \frac{1}{\pi} \int d^2\theta' \kappa(\theta') \ln |\theta - \theta'| \quad (1.21)$$

In the case of axial symmetry of SIS lens equation 1.12 simplifies to (Given on the question)

$$\psi(\theta) = 2 \int_0^\theta d\theta' \theta' \kappa(\theta') \ln \left(\frac{\theta}{\theta'} \right) \quad (1.22)$$

By substituting the values of $\Sigma(D_d\theta)$, where $D_d\theta = \xi$ from equation 1.18 and Σ_{cr} from equation 1.10 on equation 1.9, then by plugging the new expression of $\kappa(\theta)$ equation 1.22 becomes

$$\psi(\theta) = \frac{4\pi}{c^2} \frac{D_{ds}}{D_s} \sigma_v^2 \int_0^\theta d\theta' \ln \left(\frac{\theta}{\theta'} \right) \quad (1.23)$$

By integrating,

$$= \frac{4\pi}{c^2} \frac{D_{ds}}{D_s} \sigma_v^2 \left[\theta' \ln\left(\frac{\theta}{\theta'}\right) + \theta' \right] \quad (1.24)$$

$$= \theta_E (\theta \ln \theta - \theta' \ln \theta' + \theta') \quad (1.25)$$

Therefore,

$$\psi(\theta) = \theta_E \theta \quad (1.26)$$

From equation 1.13 scaled deflection angle is defined as

$$\alpha(\theta) = \nabla \psi(\theta) \quad (1.27)$$

From equations: 1.26 and 1.27,

$$\alpha(\theta) = \nabla \theta_E \theta = \theta_E \hat{\theta} \quad (1.28)$$

P.3.2: Solving the lens equation and finding the separation between images

The lens equation is given by,

$$\beta = \theta - \alpha(\theta) \quad (1.29)$$

By using the expression for scaled deflection angle for SIS from 1.28

$$\beta = \theta - \theta_E \hat{\theta} \quad (1.30)$$

or,

$$\alpha(\theta) = \beta + \theta_E \hat{\theta} \quad (1.31)$$

for $\hat{\theta} > 0$,

$$\theta_A = \beta + \theta_E \quad (1.32)$$

for $\hat{\theta} < 0$,

$$\theta_B = \beta - \theta_E \quad (1.33)$$

Thus, the separation of these images is given by,

$$\Delta\theta = \theta_A - \theta_B = \beta + \theta_E - (\beta - \theta_E) = 2\theta_E \quad (1.34)$$

P.3.3: Magnification ratio of the two images of SIS lens.

The magnification of a gravitational lens is given by,

$$\mu = (\det A)^{-1} \quad (1.35)$$

P.3.4: Time delay derivation for SIS lens as a function of θ_A and θ_B .

The time delay is given by[1]

$$c\Delta t(\beta) = (1 + z_d) \frac{D_d D_s}{D_{ds}} [\tau(\theta_A; \beta) - \tau(\theta_B; \beta)] \quad (1.36)$$

Also, from 1.14 the Format's potential is defined as,

$$\tau(\theta; \beta) = \frac{1}{2}(\beta - \alpha)^2 - \psi(\theta) \quad (1.37)$$

So,

$$\tau(\theta_A; \beta) = \frac{1}{2}(\beta - \theta_A)^2 - \psi(\theta_A) \quad (1.38)$$

By plugging the values of β and $\psi(\theta_A)$,

$$= \frac{1}{2}(\theta_A - \theta_E - \theta_A)^2 - \theta_E \theta_A \quad (1.39)$$

Therefore,

$$\tau(\theta_A; \beta) = \frac{1}{2}\theta_E^2 - \theta_E \theta_A \quad (1.40)$$

Similarly,

$$\tau(\theta_B; \beta) = \frac{1}{2}(\beta - \theta_B)^2 - \psi(\theta_B) \quad (1.41)$$

$$= \frac{1}{2}(\theta_B + \theta_E - \theta_B)^2 - \theta_E \theta_B \quad (1.42)$$

$$\tau(\theta_B; \beta) = \frac{1}{2}\theta_E^2 - \theta_E \theta_B \quad (1.43)$$

By substituting these values equation 1.36 becomes,

$$c\Delta t(\beta) = (1 + z_d) \frac{D_d D_s}{D_{ds}} \left(\frac{1}{2}\theta_E^2 - \theta_E \theta_A - \frac{1}{2}\theta_E^2 + \theta_E \theta_B \right) \quad (1.44)$$

Therefore,

$$\Delta t(\beta) = \frac{(1 + z_d)}{c} \frac{D_d D_s}{D_{ds}} \theta_E (\theta_B - \theta_A) \quad (1.45)$$

Thus, the time delay is proportional to the Einstein radius.

P.3.5: Minimum Dispersion Estimator

The minimum dispersion estimator is a simple, efficient and well tested method to estimate time delay from observed light curve[1] It helps to fine the difference between the curve at various delay times. Since it assume that light curves have the same shape but they are separated by time.

P3.6: The approximation of dispersion function near the minimum by a parabola.

The dispersion function near the minimum can be find by Taylor expanding of the functional function. i.e.

$$d^2(\lambda) = D^2(\lambda_0) + \frac{dD^2(\lambda_0)}{d\lambda}(\lambda - \lambda_0) + \frac{d^2D^2(\lambda_0)}{d\lambda^2}(\lambda - \lambda_0)^2 + 0 \quad (1.46)$$

Where, D^2 is the dispersion function and λ is the time shift. Here high order terms are negligible compared to first and second order terms.

The dispersion function is minimum at $\lambda = \lambda_0$. Now the second term of equation 1.46 goes to zero. i.e.

$$d^2(\lambda) = D^2(\lambda_0) + \frac{d^2D^2(\lambda_0)}{d\lambda^2}(\lambda - \lambda_0)^2 \quad (1.47)$$

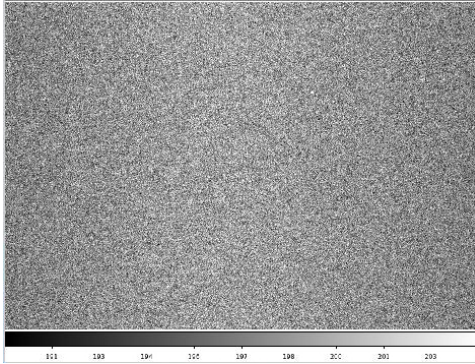
it is parabolic in shape.

1.3. Image reduction

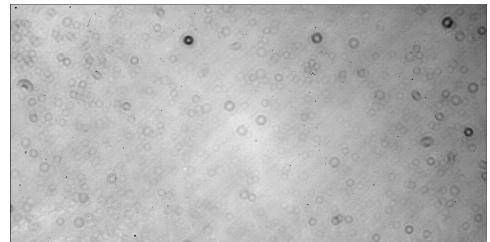
Calibration frames and science frames have been already taken. Dark frames are not provided and not necessary, since dark currents can be neglected in this case due to proper cooling. Here these images will get inspected and reduced as explained before.

1.3.1. Raw-image inspection

Calibration images are firstly visually inspected using `ds9` with `zscale` setting. Figure 1.2a and 1.2b are examples of bias and flat frames. Note that images shown here are not the whole images.



(a) Bias frame



(b) Flat frame. Color legend was unfortunately not included in screenshot.

Figure 1.2.: Calibration frames. Shown images are only central part of whole images.[†]

Average bias level is somewhat near 200. This values changes, though not so obvious in figure 1.2a, throughout the image. Left and right sides are significantly darker, meaning less bias. Presumably it is related to geometry and layout of CCD chip. Sometimes one can see quite large white dots in bias picture. Positions of these white dots vary from image to image. Because of its significant size comparing to other noises, they are mostly likely to be cosmic rays, as hinted by [1].

Middle of bias frame is chosen to calculated background and sigma, due to its lack of large-scale variation. Output of `imstats` gives us mean and sigma: 198.72 ± 2.59 . Noise here should be readout variations and random fluctuations [1].

In flat-field, most obvious feature is black circles or doughnuts. These are dusts on dewar windows and/or filter [1]. This results in lower photon counts, thus black in flat-field images. They are not on CCD chips, since they are not properly focused. Some large-scale structure can be seen. It can be explained by different quantum efficiency at different area of CCD. There are quite a lot small sharp black dots visibly. They are most likely to be bad pixels and dust directly on CCD chip.

Each flat-field has different exposure time. One can try to find correlation between mean value of image and exposure time using commands provided in [1]. Ratios between these two goes down with increasing exposure time. Firstly of all, CCD chips should be saturated here,

[†]Unfortunately some images were taken without the color/gray scale.

since with exposure time, mean values goes down. One possibility is that read-out noise in circuit gets averaged out with long exposure time, thus lower ratio.

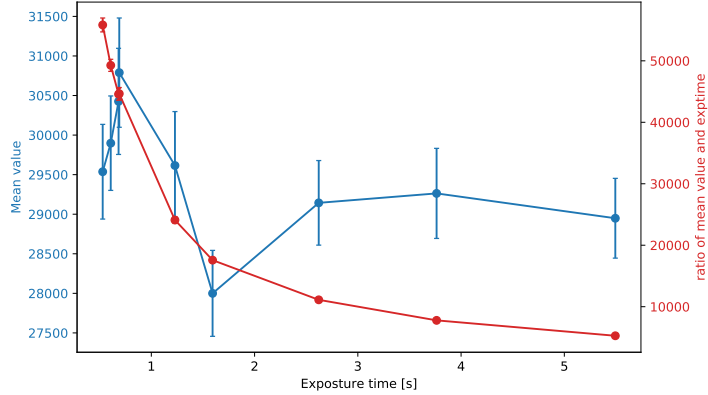


Figure 1.3.: Mean values (red) with sigmas and the ratios (blue) against exposure time of flat-field images.

In science frame one can clearly see doughnut structures and sharp black dots as in flat-field frames. Between exposure, most out-standing change would be that telescope is moving around.

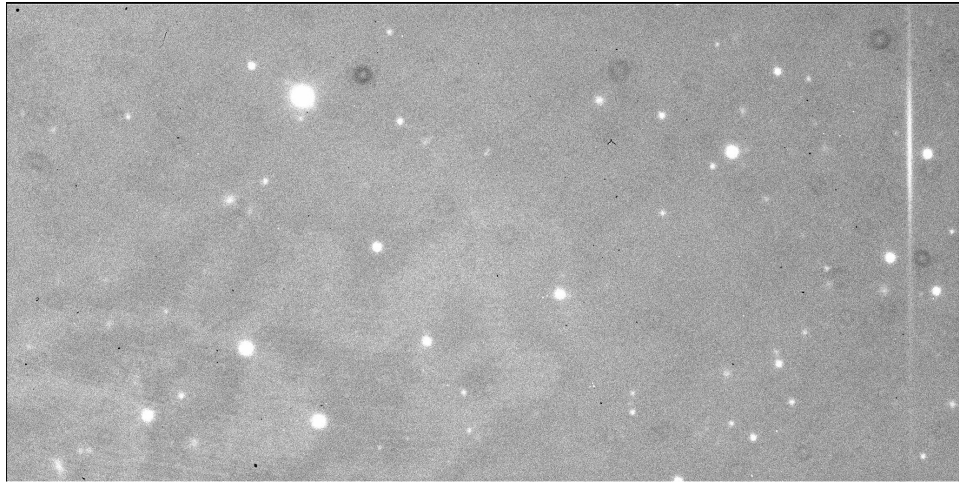


Figure 1.4.: An example of science frame.

We use `image008068.fits` as an example and compute mean and sigma in area without bright objects. Values are 693.20 ± 19.00 . It is greater than the mean value of bias frame. This is easy to understand, since science frame must contain sky.

1.3.2. Image reduction

Several science frames containing source SDSS1650+4251 are taken from one filter (R). Now these images will be reduced with help of calibrations frames and some more in `theli`. `theli` mainly consists of several tabs or processing groups. Each of following paragraph corresponds one processing group/

Initialise First off, `theli` should be properly reset and initialised. Number of CPU cores and instrument (telescope) are specified accordingly. Paths containing bias, flat, and science frames are filled in.

Preparation Through this processing group, headers contained in `.fits` files can be split and/or corrected. Comparison of headers before and after corrections reveals

- size in x and y are swapped, meaning orientation of images has been changed,
- (useless) information, e.g. comments, CCD info, Date, and etc., has been removed,
- lots of lines starting with DUMMY have been added.

They are more changes, but the listed alterations are most noticeable.

Calibration In this step, calibration frames are getting co-added. In co-addition process, images are stacked on top of each other, while making sure each object falls onto the same pixel [1]. By doing this and in the end only calibrating with co-added images, random noises will get averaged out.

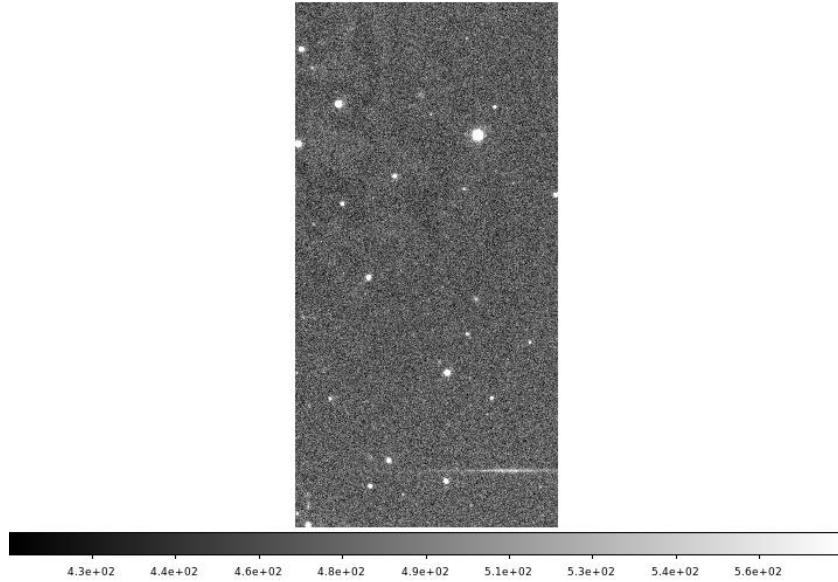
After co-addition, bias frames are free of small white dots as seen before and flat frames get a bit brighter. One can further compute noise dispersion of co-added bias frame and single bias frame. They are respectively 0.72 and 2.27. So noise level in co-added images is much lower.

The minimal value in normalised flat-field is 0. Dithering during co-addition helps to remove bright objects (stars and etc.).

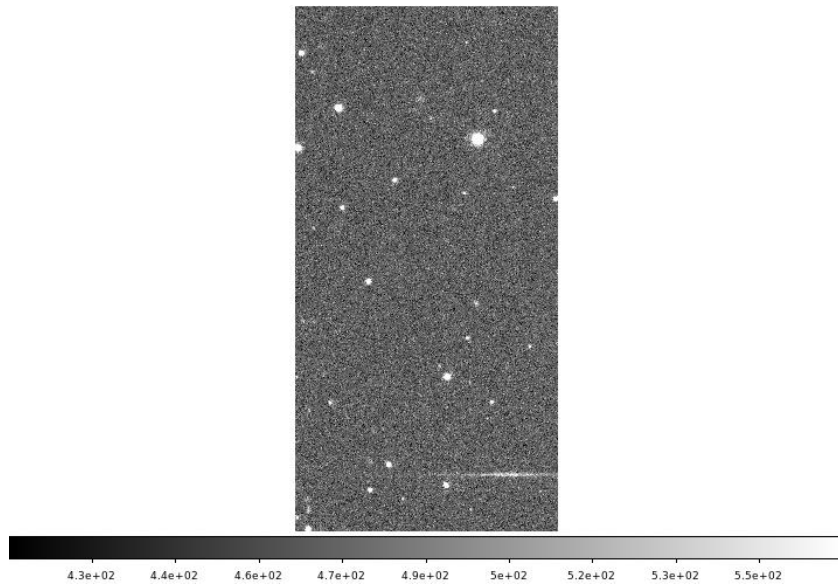
Background modelling In this processing group, only background model correction is selected, where a superflat and fringe model is created and applied. Its configurations are set according to [1]: DT = 1.0, DMIN = 10, mask expansion factor= 3, median combination, divide smoothed model, subtract fringes method, smoothing kernel for background model = 256.

In superflat, one can clearly see fringes pattern. Fringes and background sky can be extracted with smoothing process. In `SDSS1650+4251_R_block0_1_fringe.fits`, there is only fringes visible and in `SSD1650+4251_R_block0_1_illum.fits` only smooth gradient, i.e. background.

Correction given by illumination is roughly 500 (counts). Fringes are removed after correction, see figure 1.5a and 1.5b.



(a) Before correction. Pay attention to top left corner.



(b) After correction. Pay attention to top left corner.

Figure 1.5.: Background modelling

Weighting In this step, weighting and masking are performed to compensate bad pixels and different quantum efficiency. Global weights and WEIGHTS are created and applied.

Astrometry/Photometry This processing group matches dithered frame to standard astrometric coordinates and performs photometry calibration. Astrometric reference catalog is retrieved using setting provided in [1]: `Web(france)`, `SDSS-DR9`, `mag limit9|`, `radius=5'`. 421 objects are found. Then detection threshold is set to 2σ and minimal area for detection of

10 pixels.

Matching is done with `Scamp` with `DISTORT_DEGREES=1`. Calculation is done after `Scamp` has been correctly configured. After this, numerous check plots are generated.

Co-addition Frames are astrometrically co-added, subtracted by sky/background, and normalised to exposure time of 1s. Settings are again provided in [1]: `Model the sky`, `DT=1`, `DMIN=10`, `kernel width=256`, outlier rejection to 4. After co-addition, newly generated frames can be found in new folder with name starting with `coadd_`, see figure 1.6. Logically, they have the same shapes and brightest region of co-added weight frame also has high S/N ratio. Indeed, one can compute noise using `imstats` as before. RMS of region free off bright objects is 0.02, far lower than previous single frames. This can be properly understood, since frames are co-added and then normalised, resulting high S/N ratio.

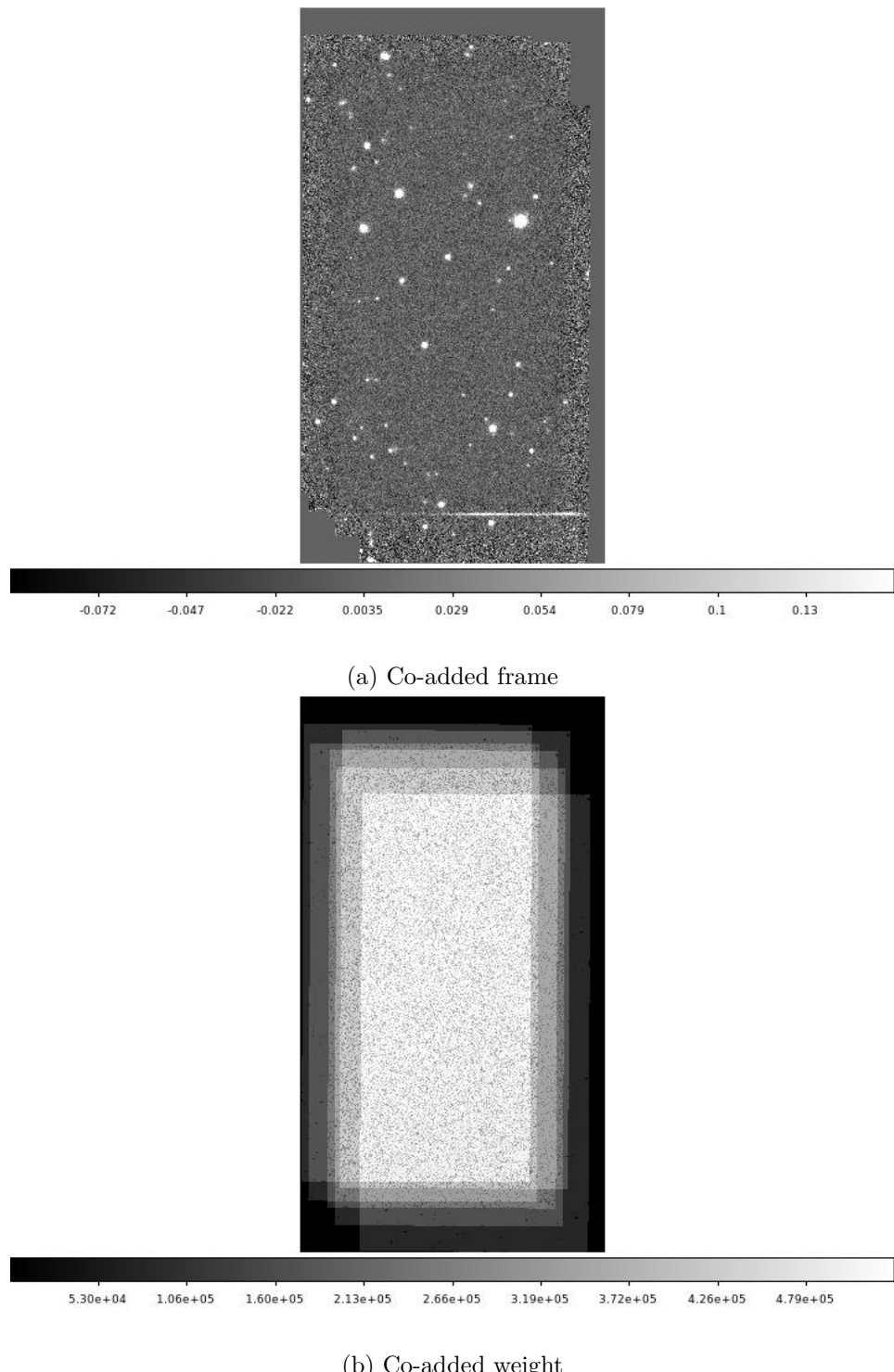


Figure 1.6.: Frames generated after co-addition

1.4. PSF extraction

In this section, point-spread-function (PSF) will be extracted. First of all, the target need to be found using standard coordinates: RA = $16^{\text{h}}50^{\text{m}}43.4^{\text{s}}$, DEC = $+42^{\circ}51'49''$.00. In `ds9`, coordinates can be turned on with `coordinate grid` option, see figure 1.7. As mentioned in [1], this target consists of two lensing images, but the separation have similar size as a typical seeing, so images are blended.

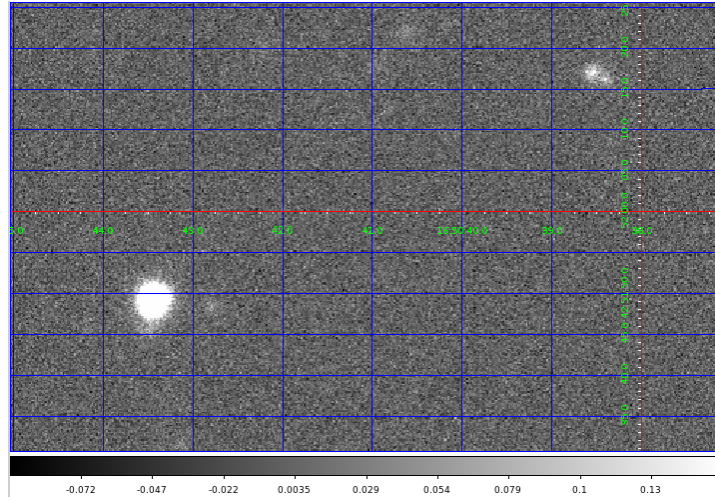
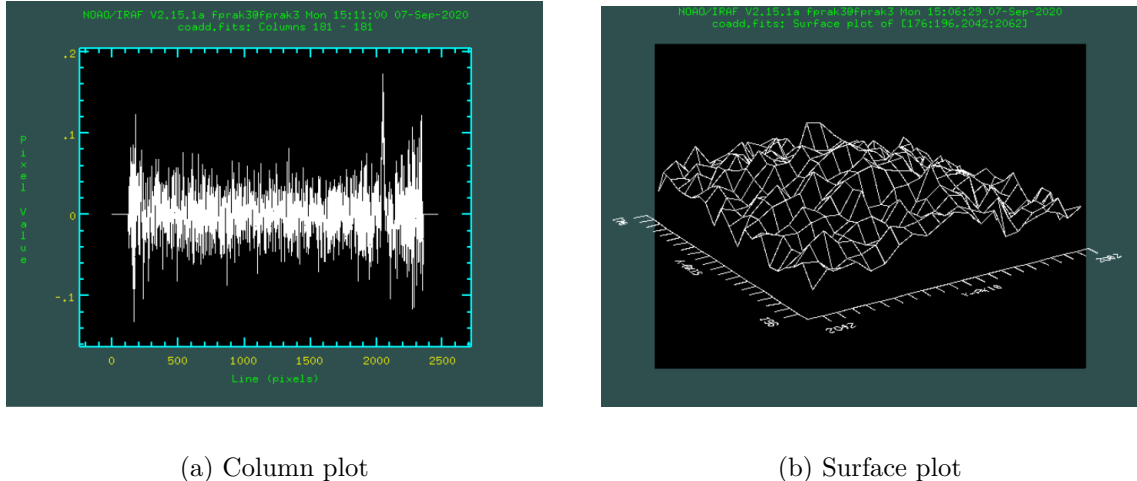


Figure 1.7.: Co-added frame with coordinate grid. Target is the left-bottom bright object.

In order to perform component fitting, PSFs of other various objects need to be extracted. One can gain more detailed information about objects using `iraf` task `imexam`.



(a) Column plot

(b) Surface plot

Figure 1.8.: Example plots of a galaxy

There are mainly two categories of objects: stars and galaxies. Since galaxies contain a number of radiation sources, their full widths at half maximum (FWHMs) are typically larger than single stars. Indeed, that is what we see. FWHMs of stars are $\sim 6 \pm 1$ pixels, of galaxies $\sim 9 \pm 1$ pixels. Identification of stars and galaxies can be easier with various plots provided by

imexam. Two example plots each are figure 1.8 and 1.9. In contour plots, stars appear to be (almost perfect) concentric circles while galaxies are messier. Radial profiles of star have clear trend while they are scattered for galaxies. These plots support previous argument regarding differentiation stars from galaxies. [seeing in arcseconds?](#)

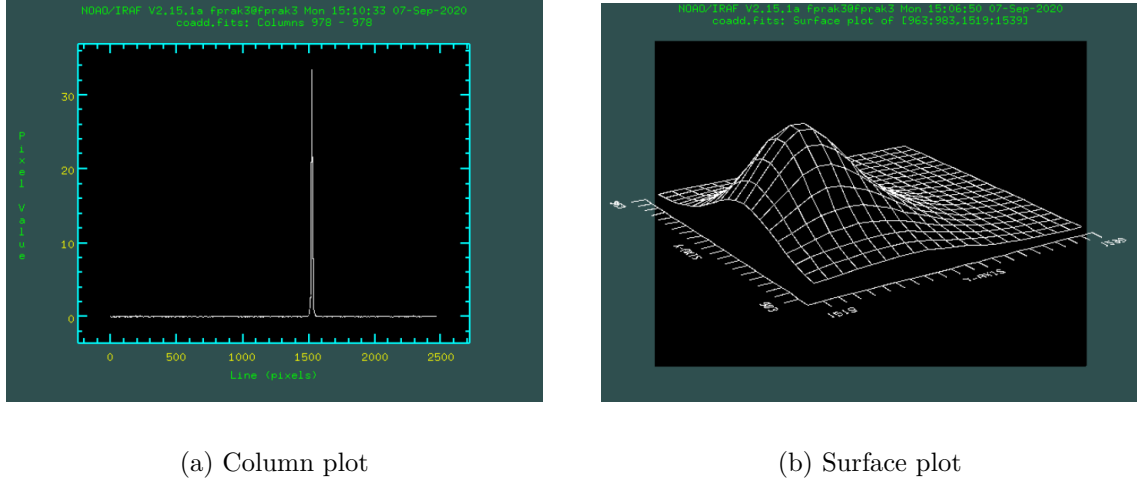


Figure 1.9.: Example plots of a star

Target contains two images, so its FWHM lies in between stars and galaxies at 8.71 pixels. Plots of target appear a bit different as well, see figure. 1.10. While surface plot do have some rough edges, column plot gives us the definite answer that this objects contains two images.

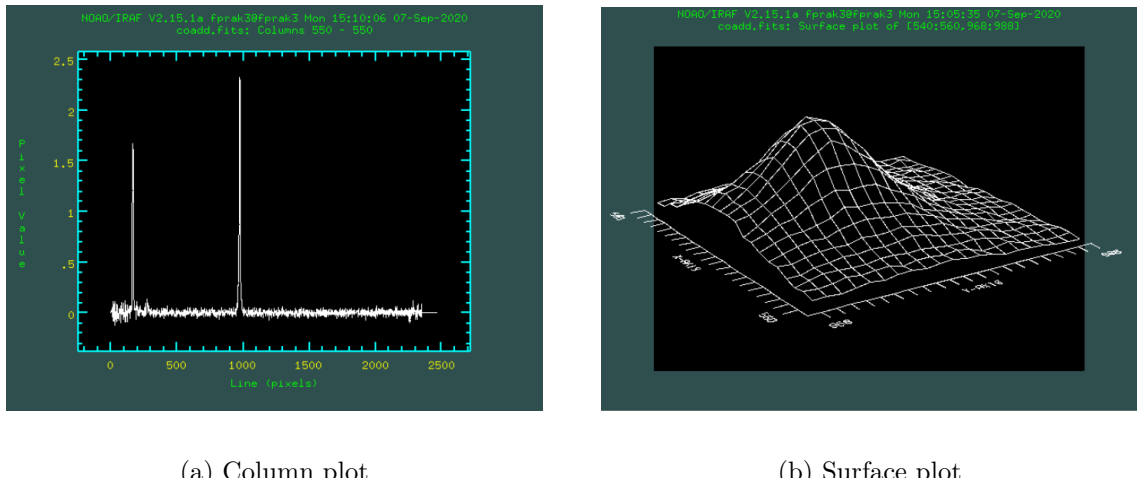
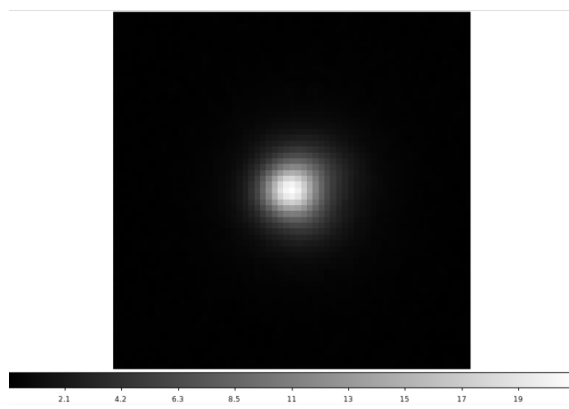


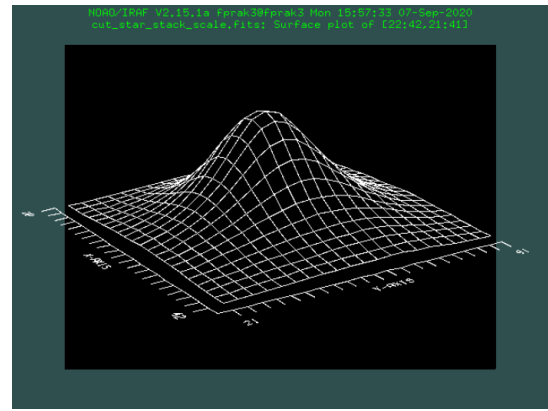
Figure 1.10.: Example plots of the target

Now to extract PSFs, a csh shell script `create_psf.csh` is used. The script takes four inputs: DIR the directory containing the images, LIST containing outputs of `imexam` of selected stars and the target, RADIUS size of square getting cut, and MAX_FWHM_STACK the maximal size of PSF. One needs to use stars, since they are quasi-point-like sources. Stars brighter (higher flux) than the target need to be included in LIST. [Why?](#) RADIUS is set to 30 pixels and MAX_FWHM_STACK to 8.5. LIST file can be found in A.1.

Outputs of `create_psf.csh` are each individual cut-outs `cut_scale*.fits` and stacked PSF `cut_star_stack_scale.fits`. Inspection of `cut_star_stack_scale.fits` shows that there is no contribution from neighbouring stars, see figure 1.11b. MFWHM of the stacked image is 8.09 as expected. Its surface plot is quite a smooth hump, even smoother than the hump of a single star. In the subsequent component fitting, the stacked image will be used, since all fluctuations/errors are averaged out.



(a) The Stacked image in ds9



(b) Surface plot of stacked image

1.5. Component fitting

Although two images are blended, one can still try to use component fitting to find out individual flux and their separation. The 2d fitting program `galfit` is used here.

`galfit` is able to fit sky value in images and sky background is important to compute the σ -image [4]. Sky value is a fit parameter in `galfit`, thus one need to compute it using `imstats` and `dfits` for normalisation: $\text{sky}=1.71 \text{ s}^{-1}$. This value is then added into the image with `ic` command provided in [1].

Input parameters of fitting are stored in `galfit.input`, listed in appendix A.2. Most important things are positions of two images, relative magnitude. These are just rough estimates as initial guess. Sky background is the third component of the fitting and sky ADU counts from previous part are given as input.

Execution of component fitting with the given parameter list outputs a log file `fit.log` and a image block, see figure 1.12. The log file contains the coordinates of two images

$$(29.69, 24.71), (31.11, 31.16)$$

magnitude difference 1.70, and $\chi^2/\nu = 44.542$. From the residuals, one can see that the fitting works properly. They are quite uniformly distributed with some fluctuation, except there is a slightly bright spot at bottom. As suggested by the tutors, it could be caused by neighbouring stars.

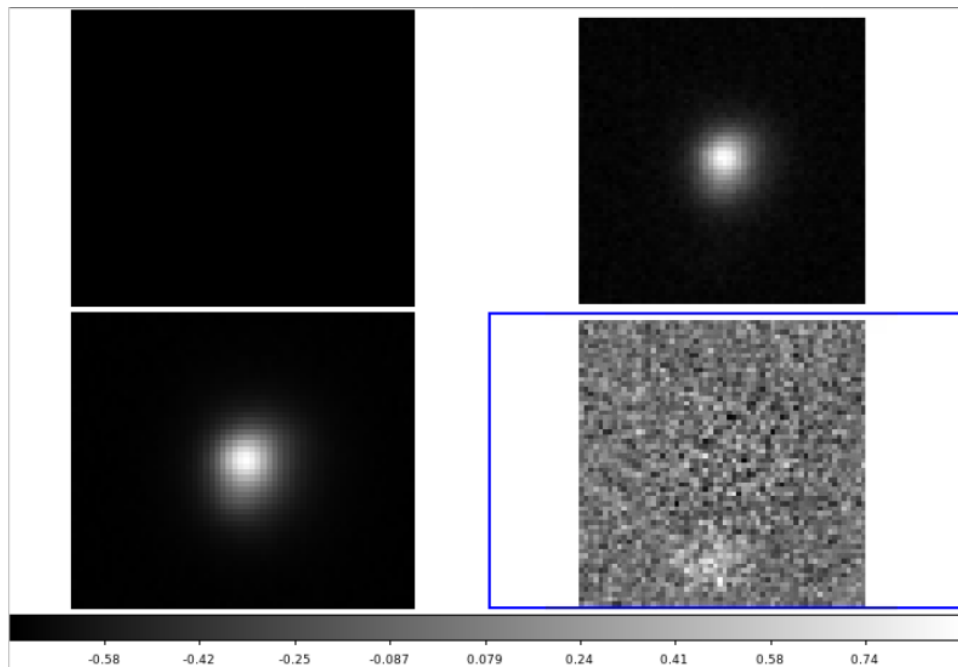


Figure 1.12.: The image block generated by `galfit` assuming there are *two* images. First image is intended to be empty. Second and third are respectively original and modelled images. Last one shows the residuals.

One could also wonder if the target could consist only of one image, since it appears to be so visually. Another fitting is done but only with two components, one PSF fit and one sky background. Resultant image block is figure 1.13. There is a clear dark spot in the residual

plot and $\chi^2/\nu = 101.615$, much worse than previous fitting. So the image cannot be explained by just one image.

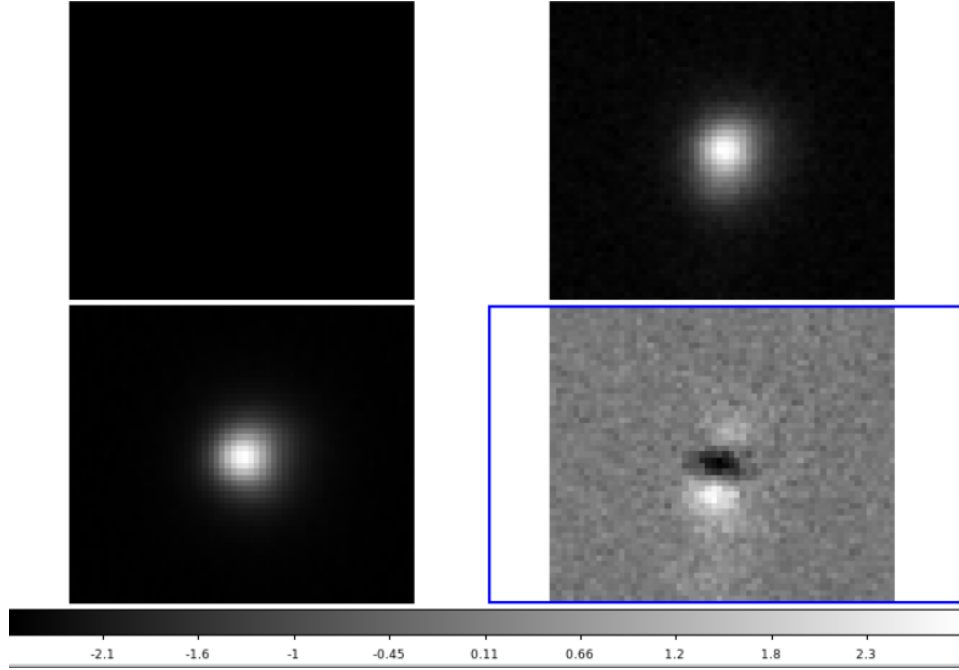


Figure 1.13.: The image block generated by galfit assuming there is only *one* image. First image is intended to be empty. Second and third are respectively original and modelled images. Last one shows the residuals.

1.6. Time-delay estimate

Time delay between two images can be estimated using minimal dispersion method. But a large number of observations are needed for it to work. Thus we take the data of [5] and the raw data are presented in appendix. A.3.

Before using minimal dispersion method, one can try to inspect the light curves visually. Figure. 1.14 shows the light curves. Most noticeable feature is a large gap between observations caused by rotation/spin of the Earth. Time delay is quite hard to discern in this plot, but if there is it should be $\mathcal{O}(10)$ days.

1.7. Lensing analysis

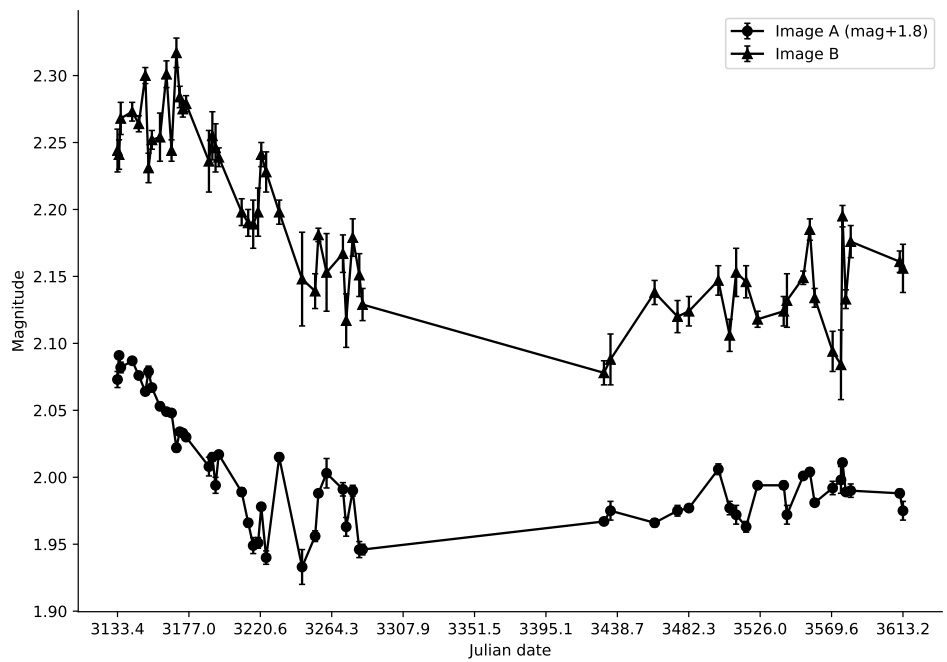


Figure 1.14.: Light curves of two images. Note that image A is originally much dimmer. For better comparison, its magnitude is added with 1.8.

2. Bad weather

A. Appendix

A.1. LIST file

COL	LINE	RMAG	FLUX	SKY	PIXELS	R	ELLIP	PA	PEAK	MFWHM
293.05	1859.53	19.30	191.3	0.15	80	3.51	0.019	82.5	3.98	7.96
435.95	1647.42	18.24	505.1	0.40	79	3.50	0.011	-63.1	10.49	8.12
974.61	1522.59	16.49	2531.7	2.10	79	INDEF	0.029	-38.3	52.22	8.16
652.00	1365.48	19.99	101.2	0.09	78	2.88	0.056	83.9	2.14	7.93
851.99	603.17	18.72	326.0	0.27	77	1.64	0.022	72.2	6.86	8.20
623.70	265.30	19.54	153.1	0.11	81	4.12	0.022	-13.9	3.18	7.88
279.06	1492.48	18.34	459.4	0.36	80	3.11	0.022	81.2	9.48	8.03
549.09	975.02	19.86	113.3	0.12	75	INDEF	0.015	68.6	2.32	8.71

A.2. galfit.input

```

# IMAGE and GALFIT CONTROL PARAMETERS
A) new_cutscale8.fits                      # Input data image (FITS file)
B) new2_cutscale8.fits                      # Output data image block (FITS file)
C) none                                       # Sigma image name (made from data if blank or "none")
D) cut_star_stack_scale.fits                 # Input PSF image (FITS file)
E) 1                                           # PSF fine sampling factor relative to data
F) none                                       # Bad pixel mask (FITS image or ASCII coord list)
G) none                                       # File with parameter constraints (ASCII file)
H) 0   60  0   60   # Image region to fit (xmin xmax ymin ymax)
I) 100  100                                # Size of the convolution box (x y)
J) 26.0                                       # Magnitude photometric zeropoint
K) 0.038  0.038                             # Plate scale (dx dy) [arcsec per pixel]
O) both                                       # Display type (regular, curses, both)
P) 0                                           # Options: 0=normal run; 1,2=make model/imgblock & quit
S) 1                                           # Modify/create objects interactively?

# INITIAL FITTING PARAMETERS
#
# column 1: Parameter number
# column 2: initial gues for value
# column 3: allow parameter to vary (yes = 1, no = 0)

```

```

# column 4: comment

# Component 1:
# PSF fit.

0) psf          # object type
1) 30 31    1 1 # position x, y [pixel]
3) 16        1   # total magnitude (only relative values are relevant)
8) 1         0   # axis ratio (<=1)
Z) 0           0   # leave in [1] or subtract [0] this comp from data?

# Component 2:
# PSF fit.

0) psf          # object type
1) 31 31    1 1 # position x, y [pixel]
3) 18        1   # total magnitude (only relative values are relevant)
8) 1         0   # axis ratio (<=1)
Z) 0           0   # leave in [1] or subtract [0] this comp from data?

# Component 3:
# sky background

0) sky          # object type
1) 1.71        1   # sky background [ADU counts]
2) 0.000       0   # dsky/dx (sky gradient in x)
3) 0.000       0   # dsky/dy (sky gradient in y)
Z) 0           0   # leave in [1] or subtract [0] this comp from data?

```

A.3. Raw data of time delay estimate

Table A.1.: Photometry of and of reference star #5, as in Fig. ???. The Julian date corresponds to HJD-2 450 000 days. The five points marked by an asterisk are not used in the determination of the time delay.

HJD	seeing ["]	mag A	σ_A	mag B	σ_B	mag star #5	$\sigma_{\text{star}\#5}$
3 133.412	1.5	0.273	0.006	2.244	0.016	-0.175	0.013
3 134.362	1.1	0.291	0.002	2.241	0.011	-0.166	0.004
3 135.385	0.9	0.282	0.004	2.268	0.012	-0.177	0.008
3 142.386	1.3	0.287	0.002	2.273	0.007	-0.167	0.003
3 146.415	1.2	0.276	0.001	2.264	0.006	-0.178	0.002
3 150.406	0.9	0.264	0.001	2.300	0.006	-0.176	0.001
3 152.367	1.0	0.279	0.004	2.231	0.011	-0.172	0.008
3 154.407	0.9	0.267	0.002	2.252	0.007	-0.175	0.003
3 159.364	1.1	0.253	0.003	2.254	0.018	-0.174	0.005
3 163.315	1.7	0.249	0.002	2.301	0.010	-0.173	0.003
3 166.425	1.0	0.248	0.002	2.244	0.008	-0.177	0.003
3 169.393	1.1	0.222	0.003	2.317	0.011	-0.189	0.006
3 171.430	1.5	0.234	0.002	2.284	0.008	-0.172	0.004
3 173.298	1.1	0.233	0.001	2.275	0.006	-0.168	0.002
3 175.300	1.1	0.230	0.001	2.279	0.006	-0.178	0.001
3 189.265	1.1	0.208	0.007	2.236	0.023	-0.172	0.012
3 191.360	1.1	0.215	0.003	2.255	0.018	-0.167	0.004
3 193.304	1.3	0.194	0.006	2.246	0.018	-0.166	0.012
3 195.252	1.0	0.217	0.002	2.239	0.007	-0.170	0.004
3 203.314*	1.4	0.186	0.001	2.345	0.007	-0.173	0.002
3 209.256	1.0	0.189	0.003	2.198	0.010	-0.167	0.007
3 213.256	1.0	0.166	0.003	2.190	0.010	-0.183	0.007
3 216.310	1.7	0.149	0.006	2.189	0.018	-0.163	0.011
3 219.281	1.6	0.151	0.004	2.198	0.018	-0.155	0.008
3 221.234	1.0	0.178	0.002	2.241	0.009	-0.179	0.003
3 224.209	1.2	0.140	0.005	2.228	0.015	-0.166	0.010
3 232.187	1.1	0.215	0.003	2.198	0.009	-0.168	0.005
3 246.163	1.3	0.133	0.013	2.148	0.035	-0.142	0.026
3 248.138*	1.5	0.172	0.004	2.054	0.013	-0.114	0.007
3 254.125	0.9	0.156	0.004	2.139	0.013	-0.160	0.007
3 256.135	1.0	0.188	0.001	2.181	0.005	-0.173	0.003
3 261.115	1.5	0.203	0.011	2.153	0.029	-0.178	0.017
3 271.109	1.3	0.191	0.005	2.167	0.014	-0.183	0.009
3 273.103	1.2	0.163	0.007	2.117	0.020	-0.176	0.013
3 277.104	1.0	0.190	0.004	2.179	0.014	-0.191	0.007
3 281.106	1.4	0.146	0.006	2.151	0.016	-0.167	0.011
3 283.100	1.2	0.146	0.004	2.129	0.012	-0.164	0.008
3 430.540	0.9	0.167	0.002	2.078	0.009	-0.135	0.003
3 434.546	0.8	0.175	0.007	2.088	0.019	-0.143	0.009
3 461.499	0.9	0.166	0.003	2.138	0.009	-0.150	0.005
3 475.491	0.9	0.175	0.004	2.120	0.012	-0.179	0.008
3 482.443	1.1	0.177	0.002	2.124	0.011	-0.149	0.004
3 500.415	1.3	0.206	0.004	2.147	0.011	-0.168	0.008
3 507.348	1.0	0.177	0.005	2.106	0.012	-0.153	0.009
3 508.403*	0.9	0.199	0.003	2.222	0.009	-0.171	0.006
3 511.303	1.0	0.172	0.007	2.153	0.018	-0.151	0.012
3 517.383	0.8	0.163	0.004	2.146	0.012	-0.168	0.007
3 524.391	0.9	0.194	0.002	2.118	0.006	-0.183	0.003
3 533.412*	1.6	0.193	0.002	2.002	0.007	-0.171	0.004
3 540.345	1.0	0.194	0.003	2.124	0.011	-0.168	0.006
3 542.323	1.1	0.172	0.007	2.132	0.020	-0.194	0.014
3 552.291	0.9	0.201	0.00123	2.149	0.005	-0.179	0.001
3 556.295	0.9	0.204	0.003	2.185	0.008	-0.176	0.005
3 559.280	1.0	0.181	0.002	2.134	0.007	-0.160	0.004
3 564.295*	1.3	0.228	0.001	2.300	0.007	-0.167	0.003
3 570.247	1.0	0.192	0.005	2.094	0.015	-0.165	0.010

HJD	seeing ["]	mag A	σ_A	mag B	σ_B	mag star #5	$\sigma_{\text{star}\#5}$
3 575.323	1.3	0.198	0.010	2.084	0.026	-0.172	0.019
3 576.264	1.0	0.211	0.001	2.195	0.008	-0.181	0.002
3 578.275	1.2	0.189	0.002	2.133	0.007	-0.177	0.003
3 581.284	1.2	0.190	0.005	2.176	0.012	-0.188	0.009
3 611.225	1.2	0.188	0.003	2.161	0.008	-0.165	0.005
3 613.201	1.5	0.175	0.007	2.156	0.018	-0.180	0.013

Bibliography

- [1] Unknown. *Advanced lab course in physics at Bonn University: Optical Astronomy and Gravitational Lensing*. 2020.
- [2] Edward W. Kolb and Michael S. Turner. *The Early Universe*. Addison-Wesley, 1993.
- [3] P. Schneider. *Introduction to Gravitational Lensing and Cosmology*.
- [4] Chien Y. Peng. *GALFIT USER'S MANUAL*. URL: <https://users.obs.carnegiescience.edu/peng/work/galfit/README.pdf>.
- [5] C. Vuissoz et al. “COSMOGRAIL: the COSmological MOnitoringof GRAVItational Lenses”. In: (2006).